

Downmodulation of the Inflammatory Response to Bacterial Infection by $\gamma\delta$ T Cells Cytotoxic for Activated Macrophages

By Paul J. Egan and Simon R. Carding

From the Department of Clinical Studies, School of Veterinary Medicine, University of Pennsylvania, Philadelphia, Pennsylvania 19104

Abstract

Although $\gamma\delta$ T cells are involved in the regulation of inflammation after infection, their precise function is not known. Intraperitoneal infection of T cell receptor (TCR)- $\delta^{-/-}$ mice with the intracellular bacterium *Listeria monocytogenes* resulted in the development of necrotic foci in the livers. In contrast, the peritoneal cavities of infected TCR- $\delta^{-/-}$ mice contained an accumulation of low density activated macrophages and a reduced percentage of macrophages undergoing apoptosis. $\gamma\delta$ T cell hybridomas derived from mice infected with *Listeria* were preferentially stimulated by low density macrophages from peritoneal exudates of infected mice. Furthermore, primary splenic $\gamma\delta$ T cells isolated from *Listeria*-infected mice were cytotoxic for low density macrophages in vitro, and cytotoxicity was inhibited in the presence of antibodies to the $\gamma\delta$ TCR. These results demonstrate a novel interaction between $\gamma\delta$ T cells and activated macrophages in which $\gamma\delta$ T cells are stimulated by terminally differentiated macrophages to acquire cytotoxic activity and which, in turn, induce macrophage cell death. This interaction suggests that $\gamma\delta$ T cells regulate the inflammatory response to infection with intracellular pathogens by eliminating activated macrophages at the termination of the response.

Key words: T lymphocyte • macrophages • apoptosis • inflammation • cell-mediated immunity

Introduction

Resistance to infection by intracellular microbes involves a series of interactions between cells of the immune system, of which the activated macrophage is central (1, 2). It can respond to, and secrete, a variety of cytokines that control key events in the initiation, resolution, and repair processes of inflammation and mediate the phagocytosis and destruction of infectious pathogens. In contrast, activated macrophages can also directly contribute to tissue injury through the release of toxic enzymes and proinflammatory cytokines (3–5). Regulation of macrophage activation must therefore be tightly regulated to achieve destruction of the invading pathogen while reducing the amount of damage to host tissues. The existence of such mechanisms is made clear by the observation that even massive cellular reactions and macrophage accumulation in tissues such as that seen in lobar pneumococcal pneumonia (6) can be resolved completely without obvious residual tissue injury. The importance of regulating the effects of macrophage activation is emphasized by the continued macrophage accumulation

that is a hallmark feature of many chronic inflammatory diseases such as emphysema, asthma, glomerulonephritis, various forms of arthritis, myocardial infarction, and atheroma. Macrophages have been shown to undergo apoptosis in vitro in a manner analogous to polymorphonuclear neutrophils in response to a variety of stimuli (7–10). However, it is not clear if this mechanism of macrophage clearance occurs in vivo (11) and, if it does, how it is mediated and regulated.

Recent experiments have demonstrated that $\gamma\delta$ T cells play an active role in the regulation and resolution of inflammatory processes associated with infectious disease and autoimmunity. They have been shown to accumulate in sites of inflammation associated with infections with viruses such as influenza and Sendai virus (12, 13) or parasitic infections such as malaria and *Toxoplasma gondii* (14, 15). Mice deficient in $\gamma\delta$ T cells (TCR- $\delta^{-/-}$ mice) exhibited exaggerated tissue inflammation and necrosis after infection with bacteria such as *Listeria monocytogenes* (16, 17) or *Mycobacterium tuberculosis* (Mtb)¹ (18) or parasites such as *Eimeria*

Address correspondence to Simon R. Carding at his present address, The University of Leeds, School of Biochemistry and Molecular Biology, Leeds LS2 9JT, W. Yorkshire, England, UK. Phone: 44-0113-233-1404; Fax: 44-0113-233-1421; E-mail: S.R.Carding@bmb.leeds.ac.uk

¹Abbreviations used in this paper: FSC, forward scatter; hsp60, heat shock protein 60 kD; Mtb, *Mycobacterium tuberculosis*; PECs, peritoneal exudate cells; PI, propidium iodide; SSC, side scatter.

veriformis (19). Although mice depleted of $\gamma\delta$ T cells are able to clear *Listeria* when given low doses of bacteria, they succumb to infection with higher doses of *Listeria*. Increased mortality in the absence of $\gamma\delta$ T cells, however, is due to liver failure as a result of uncontrolled hepatocyte necrosis rather than overwhelming bacterial infection in these mice (16). In addition, $\gamma\delta$ T cells have been shown to accumulate in inflammatory lesions associated with experimental models of autoimmune diseases such as lupus (20), rheumatoid arthritis (21), and orchitis (22). Despite these provocative findings, however, the precise mechanisms by which $\gamma\delta$ T cells may regulate the inflammatory response and whether or not they can interact with or influence the fate of activated macrophages has not been defined.

We have addressed this question using the mouse model of listeriosis. Many of the paradigms of infection and cell-mediated immunity, particularly the central role of activated macrophages, have been established using this model (23). After experimental infection of mice with *Listeria*, bacteria are rapidly phagocytosed by resident macrophages such as Kupffer cells in the liver. This is followed by an early phase of neutrophil and monocyte influx in the first 24–48 h that form granulomatous lesions at the site of infection. Experimental infection with *Listeria* was also one of the first experimental systems in which the involvement of $\gamma\delta$ T cells in pathogen-induced immune responses was demonstrated (24, 25). $\gamma\delta$ T cells respond during murine listeriosis by expanding in the spleen, liver, or peritoneal cavity after intravenous or intraperitoneal infection. The kinetics of the $\gamma\delta$ T cell response are controversial. Whereas some reports have described an early (day 1–3) $\gamma\delta$ T cell response (24, 26), others have shown that $\gamma\delta$ T cells respond late in the course of infection when the number of recoverable, viable bacteria is in decline (25). These differences may be related to the dose of bacteria given or the site of infection (27). A late $\gamma\delta$ T cell response, however, also occurs after viral infection of mice (12), which peaks after viral clearance and is consistent with the hypothesis that $\gamma\delta$ T cells are involved in the resolution of inflammation. Responding $\gamma\delta$ T cells predominantly express either V δ 6.3 or V δ 4 TCR chains (27), a population that comprises the predominant $\gamma\delta$ T cell population found circulating through blood and peripheral lymphoid tissues (28). These receptors have also been previously shown to be expressed by $\gamma\delta$ T cells that react with the 60-kD heat shock protein 60 (hsp60, cpn60) of *Mtb* (29).

Evidence for a requirement for $\gamma\delta$ T cells in the resolution of the cellular response to *Listeria* and prevention of chronic inflammation has been obtained from infection of mice rendered deficient of $\gamma\delta$ T cells by gene targeting or by administering mAbs to the $\gamma\delta$ TCR (16, 17). Clearance of bacteria occurs as efficiently in $\gamma\delta$ T cell-depleted mice as it does in wild-type controls. Secondary responses to infection with *Listeria* were also unimpaired in $\gamma\delta$ T cell-deficient mice, demonstrating that $\gamma\delta$ T cells are not involved in bacterial clearance or in the generation of T cell memory. However, $\gamma\delta$ T cell-deficient mice demonstrate exaggerated inflammation, liver necrosis, and associated second-

ary inflammation, which is not seen in wild-type or $\alpha\beta$ T cell-deficient mice. The observation that $\gamma\delta$ T cells, when adoptively transferred to SCID mice, can abrogate the tissue injury that results from subsequent *Listeria* infection (16) demonstrates that $\gamma\delta$ T cells are both necessary and sufficient to prevent excessive inflammatory responses and tissue necrosis. However, despite this evidence that $\gamma\delta$ T cells are involved in the response to infection with *Listeria* as well as other intracellular pathogens, very little is known about the nature of the cells they react with after infection and how $\gamma\delta$ T cells can prevent chronic inflammation.

Here, we demonstrate that intraperitoneal infection of TCR- $\delta^{-/-}$ mice results in a massive accumulation of low density, activated macrophages at the site of infection. This accumulation of activated macrophages is associated with decreased levels of apoptotic cell death. We also show that these macrophages are stimulatory for $\gamma\delta$ T cells and are lysed *in vitro* by primary $\gamma\delta$ T cells as a result of TCR-mediated recognition of, and activation by, the macrophages. Based on these data, we propose that a function of $\gamma\delta$ T cells is to downregulate the response of inflammatory macrophages after infection by inducing activated macrophages to undergo apoptosis and return the animal to a state of normal macrophage homeostasis, thus preventing the development of chronic inflammation.

Materials and Methods

Mice. C57BL/6 wild-type, C57BL/6 TCR- $\delta^{-/-}$, C57BL/6 TCR- $\beta^{-/-}$, and BALB/c mice were purchased from The Jackson Laboratory and were used between 6 and 10 wk of age.

Separation of Peritoneal Exudate Cells from *Listeria*-infected Mice. *L. monocytogenes* strain 10403S was used for all experiments. Frozen aliquots of bacteria were stored at -80°C before infection. Unless otherwise stated, mice were infected with 2×10^4 CFU per mouse intraperitoneally for 6 d. Peritoneal exudate cells (PECs) were obtained by two rounds of peritoneal lavage with 5 ml of HBSS containing 10 U/ml heparin. PECs were fractionated by centrifugation over two discontinuous Percoll columns in siliconized tubes as described previously (30). For the first fractionation, cells were spun over a column comprised of a 43 and 63% Percoll. For the second Percoll fractionation, the cells that had collected at the interface between the 43 and 63% Percoll were centrifuged over a column comprised of 48 and 58% Percoll. Fractionated cells were used for cytocentrifuge preparations, stained for flow cytometry, or cultured with primary splenic $\gamma\delta$ T cells or $\gamma\delta$ T cell hybridomas.

Generation of T Cell Hybridomas. $\gamma\delta$ T cell hybridomas were generated essentially as described previously (29). C57BL/6 TCR- $\beta^{-/-}$ mice or BALB/c mice were infected with 2×10^4 CFU *Listeria* intravenously. To increase the proportion of $\gamma\delta$ T cells present in the fusion, BALB/c mice were depleted of $\alpha\beta$ T cells by injecting them with 200 μg of H57-597 antibody 2 d before and 3 d after infection. Splenocytes were harvested on day 6 of infection and cultured for 3 d in DMEM media containing 10% (vol/vol) FCS, 100 U/ml penicillin, 100 $\mu\text{g}/\text{ml}$ streptomycin, 2 mM l-glutamine, 0.1 mM nonessential amino acids, 1 mM sodium pyruvate, MEM vitamin solution (GIBCO BRL), and 2×10^{-5} M 2-ME in the presence of 5 $\mu\text{g}/\text{ml}$ Con A. At the end of the culture period, splenocytes were fused with the thymoma line BW 5197 TCR- $\alpha^{-}\beta^{-}$ and grown under selection in hypo-

xanthine and azoserine. Hybrids were screened for expression of the $\gamma\delta$ TCR by flow cytometry, and positive cells were cloned at least three times by limiting dilution. TCR gene expression was determined by PCR amplification of the junctional regions of the γ and δ chain genes as described previously (29) and where possible by flow cytometry using TCR V region-specific antibodies. Hybridoma cells were analyzed for IL-2 production by culturing 10^5 cells overnight in the presence of $10 \mu\text{g/ml}$ plate-bound anti-CD3 antibody (clone 500-A2; Caltag Labs.) and assaying the culture supernatant by ELISA using a matched pair of IL-2-specific mAbs (PharMingen).

Flow Cytometric Analysis. Peritoneal cells or $\gamma\delta$ T cell hybridomas were analyzed by flow cytometry on a FACScan™ flow cytometer using CELLQuest™ software (Becton Dickinson). Cells were stained with antibodies to the following molecules: FITC-conjugated antibodies to Mac-1 (clone M1/70), $\alpha\beta$ TCR (clone H57-597), GR-1 (clone RB6-8C5), and PE-conjugated antibodies to $\gamma\delta$ TCR (clone GL3), F4/80, and B220 (RA3-6A2), all from Caltag Labs. In some experiments, $\gamma\delta$ T cell hybridomas were also stained with an FITC-conjugated antibody to V δ 4 (GL2; PharMingen) or a biotinylated antibody to the V δ 6.3 chain of the $\gamma\delta$ TCR (17C; reference 27), followed by streptavidin-PE (Caltag Labs.). Intracellular IFN- γ was detected using PE-conjugated anti-IFN- γ antibody (clone XMG1.2; PharMingen) as previously described (31). Cells were fixed with 1% paraformaldehyde for 1 h and permeabilized with 0.1% saponin in PBS containing 2% FCS. For all staining experiments, isotype-matched antibodies of irrelevant specificity were used to determine the level of nonspecific staining and frequency of cells stained with test antibodies. Additional negative controls used to confirm specificity of intracellular cytokine staining were the staining of fixed but not permeabilized cells, as well as preincubation of permeabilized cells with native anti-IFN- γ antibody to abolish staining. Analysis of apoptotic cells by annexin binding was carried out using an apoptosis detection kit containing annexin-FITC and propidium iodide (PI) (R & D Systems, Inc.) according to the manufacturer's instructions. A FACStar™ flow cytometer (Becton Dickinson) was used for cell sorting.

Stimulation of Hybridomas. Hybridoma cell cultures containing at least 70% TCR⁺ cells were labeled with $5 \mu\text{M}$ of the inert fluorescent dye, carboxy-fluorescein succinimidyl ester (CFSE; Molecular Probes), before culture as described previously (32). Labeled cells (2×10^4) were cultured in the presence or absence of 10^5 PECs for 48 h. For the detection of intracellular IFN- γ production, cells were cultured with $2 \mu\text{M}$ monensin for the last 4 h of the culture period.

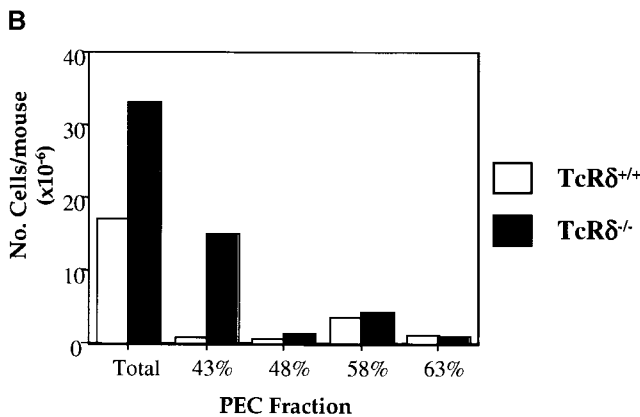
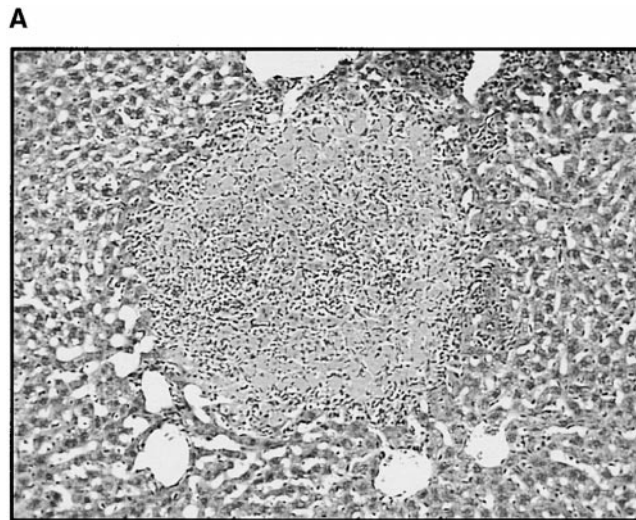
⁵¹Cr-Release Assay. PECs were harvested from TCR- $\delta^{-/-}$ mice infected 6 d previously with *Listeria* and fractionated over 43% Percoll to separate low density macrophages from higher density cells. Splenocytes from wild-type, TCR- $\beta^{-/-}$, and TCR- $\delta^{-/-}$ mice were depleted of B cells, $\alpha\beta$ T cells, and myeloid cells by immunomagnetic cell sorting, performed by labeling of the cells with the biotinylated mAbs H57 (anti- $\alpha\beta$ TCR), RA3 (anti-B220), and M1/70 (anti-Mac-1), followed by passage over a streptavidin-microbead column (Miltenyi Biotec). In some experiments, splenocytes from 6 d *Listeria*-infected mice were first depleted of B cells by passage of cells over nylon wool columns. F(ab)₂ fragments of the mAb GL3, specific to the $\gamma\delta$ TCR, were prepared by American Qualex and included in the cultures at the concentrations shown (see Fig. 6). F(ab)₂ fragments of hamster IgG were used as a control. Low or high density PECs were labeled with ⁵¹Cr, and 10^5 cells were cultured with effector T cells at the various E/T cell ratios for 16 h. After culture, re-

leased ⁵¹Cr was quantified by counting $100 \mu\text{l}$ of supernatant in a gamma counter. Specific lysis was calculated according to the following formula: specific lysis = (experimental lysis – spontaneous lysis)/(total lysis – spontaneous lysis) \times 100%.

Results

Experimental Design. Although infection of TCR- $\delta^{-/-}$ with low doses of *Listeria* results in a self-resolving infection, these mice develop tissue necrosis at sites of infection. In contrast, infection of TCR- $\delta^{-/-}$ mice with higher doses of *Listeria*, which can still be cleared from wild-type mice, results in catastrophic liver damage and death (16, 17). We therefore investigated potential regulatory functions of $\gamma\delta$ T cells during the inflammatory response to infection. Previous analyses of the consequences of the absence of $\gamma\delta$ T cells during *Listeria* infection have concentrated on pathological responses in the liver. As activated macrophages are a major source of soluble inflammatory mediators that contribute to tissue necrosis, we decided to investigate the effects of listeriosis in TCR- $\delta^{-/-}$ mice in the peritoneum, which provides an accessible source of activated macrophages. TCR- $\delta^{-/-}$ mice were infected via the intraperitoneal route with 2×10^4 CFU *Listeria*, strain 10403S. (LD₅₀ for wild-type C57BL/6 mice is 3×10^5 CFU.) At this dose, TCR- $\delta^{-/-}$ mice clear the bacteria but develop necrotic liver lesions.

Infection of TCR- $\delta^{-/-}$ Mice with *Listeria* Results in the Accumulation of Low Density, Activated Macrophages in the Peritoneum. Infection of wild-type mice with *Listeria* induces an expansion and activation of $\gamma\delta$ T cells at the site of infection that peaks 6 d after infection (25, 27, 33). PECs and livers were therefore harvested from wild-type and TCR- $\delta^{-/-}$ mice 6 d after intraperitoneal infection with 2×10^4 viable *Listeria*. In the livers of wild-type mice, $\gamma\delta$ T cells increase in number by more than 10-fold, reaching maximal levels 6 d after infection, at which time they also outnumber $\alpha\beta$ T cells (34). The $\gamma\delta$ T cell response is dominated by V δ 6.3 and V δ 4 receptor-bearing cells, and it is paralleled by the monocyte/macrophage response, which peaks 6 d after infection in the livers of these animals (27, 34). In TCR- $\delta^{-/-}$ mice 6 d after infection, the sections of liver showed disruption of the normal granulomatous and PMN response and excessive hepatocyte necrosis (Fig. 1 A). The excessive PMN response was characterized by the accumulation of neutrophils (data not shown) and macrophages (Fig. 1). A similar abnormal PMN response and accumulation of activated macrophages was also seen in the spleens of TCR- $\delta^{-/-}$ mice (our unpublished observations). Although TCR- $\delta^{-/-}$ mice show increased susceptibility to infection with high infectious doses of *Listeria*, the bacterial burden was not significantly higher compared with wild-type mice, and bacteria were not detectable within the liver lesions or hepatocytes. TCR- $\delta^{-/-}$ mice, however, do have increased serum concentrations of ammonia and aminotransferases, indicating that death of the TCR- $\delta^{-/-}$ mice is due to overwhelming liver necrosis and organ failure (data not shown and reference 16).



We compared liver pathology with that seen in the peritoneal cavity after infection. After 6 d of infection, the total number of PECs recovered from TCR- $\delta^{-/-}$ mice was increased approximately twofold compared with age- and sex-matched wild-type controls (Fig. 1 B). Flow cytometric analysis of PECs revealed an increase in the percentage of Mac1⁺ and F4/80⁺ macrophages in the peritoneum, although the composition of other cell subsets was not changed (Fig. 1 C). As peritoneal monocytes/macrophages can have distinct phenotypic and functional properties depending on the state of maturation and/or activation, they were separated by density over discontinuous Percoll gradients to obtain more homogeneous macrophage populations (30). Cells were collected from the interface of 43, 48, and 58% Percoll. After centrifugation of the cells over Percoll, the increase in PEC numbers in TCR- $\delta^{-/-}$ mice after infection was almost totally accounted for by a 15–20-fold increase in the number of cells migrating to the 43% Percoll interface (Fig. 1 B). These cells were predominantly macrophages, as assessed by staining with antibodies to Mac-1 and F4/80 (Fig. 1 C). In contrast, there were no significant differences in the number of PECs from any of the higher density Percoll fractions (Fig. 1 B) or cell pellet ($1.0\text{--}1.2 \times 10^7$ cells in TCR- $\delta^{+/+}$ and TCR- $\delta^{-/-}$).

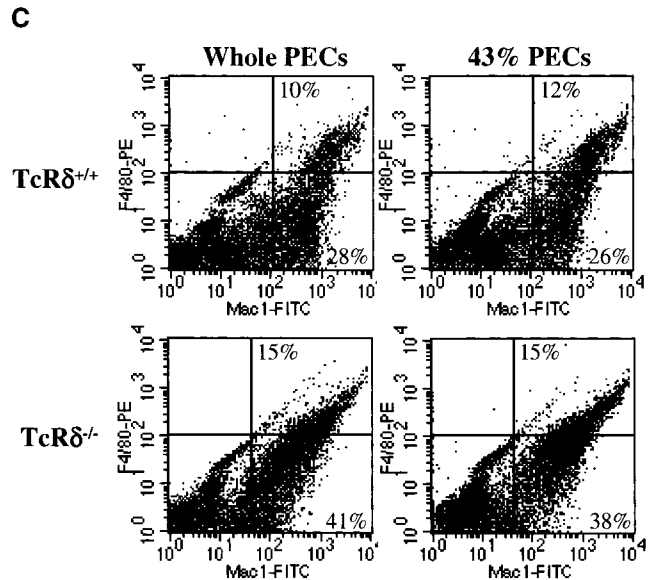


Figure 1. Exacerbated inflammatory responses in TCR- $\delta^{-/-}$ mice after infection with *Listeria*. Wild-type or TCR- $\delta^{-/-}$ mice were infected with 2×10^4 CFU for 6 d. (A) Necrotic lesion in the liver after infection. Paraffin sections were stained with hematoxylin and eosin. Magnification 250. (B) Activated, low density macrophages accumulate in the peritoneum of *Listeria*-infected TCR- $\delta^{-/-}$ mice. Wild-type (TCR- $\delta^{+/+}$) and $\gamma\delta$ T cell-deficient (TCR- $\delta^{-/-}$) mice were infected with *Listeria*, and PECs were collected 6 d later. PECs were fractionated by centrifugation over discontinuous Percoll gradients, and cells were collected at the interfaces of 43, 48, 58, and 63% Percoll. (C) Expression of macrophage markers by PECs from wild-type or TCR- $\delta^{-/-}$ mice after infection. Whole PECs or PECs separated by centrifugation over 43% Percoll were stained for the macrophage markers Mac-1 and F4/80. The percentages of positive cells in each quadrant are shown. The results shown are typical of five independent experiments.

Decreased Apoptosis of Low Density Macrophages in the Absence of $\gamma\delta$ T Cells after Infection with Listeria. One possibility to account for the accumulation of low density, activated macrophages in the peritoneum of *Listeria*-infected TCR- $\delta^{-/-}$ mice is the absence or failure of clearance mechanisms. To test this hypothesis, PEC cell fractions from day 6 infected wild-type and TCR- $\delta^{-/-}$ mice were evaluated for viable and dying cells by staining with annexin-FITC and PI (Fig. 2). The percentage of apoptotic PECs from wild-type mice was approximately twofold higher compared with PECs from the TCR- $\delta^{-/-}$ mice. This was true for both annexin-positive, PI-negative (apoptotic) cells and annexin-positive, PI-positive (necrotic) cells. Although the 43% PEC fraction was enriched for apoptotic cells, there was a significant decrease in the percentage of both apoptotic and necrotic cells from the TCR- $\delta^{-/-}$ mice compared with cells from the wild-type mice. Taking into account the 15-fold increase in low density macrophages and the two-fold decrease in the percentage of apoptotic and necrotic cells present in the peritoneum of infected TCR- $\delta^{-/-}$ mice, there are $\sim 20\text{--}30$ -fold more viable, activated macrophages present in these animals compared with wild-type mice.

The 48% PEC fraction from wild-type mice contained significantly more necrotic cells, but there was no signifi-

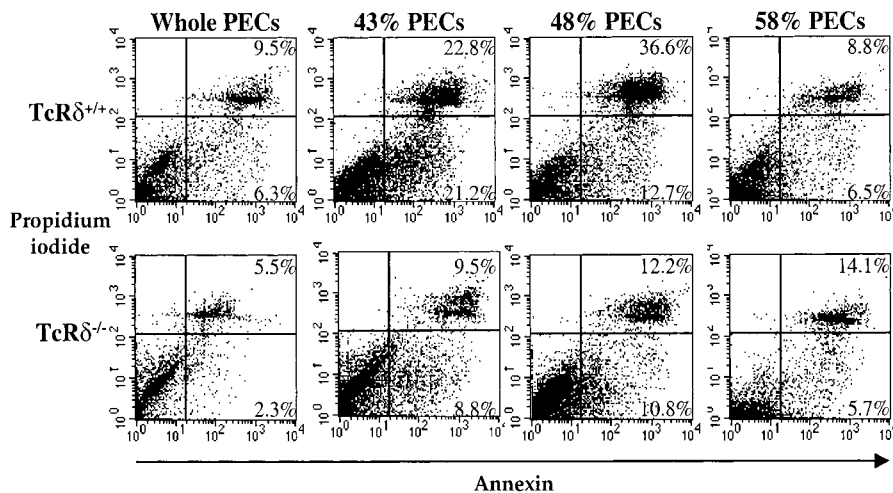


Figure 2. Reduced apoptosis and death of PECs from TCR- $\delta^{-/-}$ mice after infection with *Listeria*. Wild-type (TCR- $\delta^{+/+}$) and $\gamma\delta$ T cell-deficient (TCR- $\delta^{-/-}$) mice were infected with *Listeria*, and 6 d later, PECs were collected, fractionated over Percoll gradients, and stained with annexin-FITC and PI to distinguish viable and dying cells (B). The results shown are typical of those obtained from three independent experiments.

cant difference in the percentage of apoptotic cells. No differences were detected in the percentage of apoptotic or necrotic cells in the 58% PEC fraction or in the cell pellet (data not shown). These results suggest an interaction between $\gamma\delta$ T cells and low density, activated macrophages at the end of the response to infection with *Listeria*, resulting in the death of these macrophages. In the absence of $\gamma\delta$ T cell killing, activated macrophages accumulate in the peritoneum of infected mice.

Derivation of $\gamma\delta$ T Cell Hybridomas from *Listeria*-infected Mice. To examine the ability of the PEC fractions to stimulate $\gamma\delta$ T cells, it was necessary to obtain clonal populations of $\gamma\delta$ T cells that had responded to infection with *Listeria*. Accordingly, we derived a panel of $\gamma\delta$ T cell hybridomas from splenocytes of mice infected with *Listeria*. $\gamma\delta$ T cells were obtained from spleens of BALB/c or C57BL/6 (TCR- $\beta^{-/-}$) mice infected 6 d previously, which corresponds to the peak of the $\gamma\delta$ T cell response in vivo (27). These cells were expanded in vitro for 3 d and then fused to the BW 5197 TCR- $\alpha^{-}\beta^{-}$ thymoma cell line. Hybrids were screened by flow cytometry for the expression of $\gamma\delta$ TCRs and positive cells cloned by limiting dilution. Receptor gene usage was determined by reverse transcriptase-PCR analysis of mRNA isolated from the hybridomas using PCR primers spanning the junction regions of rearranged γ and δ chain genes and, where possible, by staining the hybridomas with antibodies against specific receptor chains.

A panel of 11 $\gamma\delta$ TCR $^{+}$ hybridomas was derived from C57BL/6 mice, and 3 were from BALB/c mice (Table I). Analysis of TCR gene usage showed that all hybridomas expressed the V γ 1 TCR chain, whereas 11 of the 14 hybridomas expressed either the V δ 6.3 or the related V δ 6 λ 12 chain. In addition, another hybridoma expressed the V δ 4 chain. Receptor usage by the hybridomas correlated with the predominance of V δ 6.3 $^{+}$ T cells among $\gamma\delta$ T cells that respond to *Listeria* infection in vivo (27). Expression of the $\gamma\delta$ TCR on the surfaces of hybridomas was not stable, and cells maintained in culture frequently lost expression. Hybridomas were therefore thawed from frozen stocks not

more than 1 wk before stimulation experiments, and cells were screened for receptor expression before use in all experiments. Cultures containing <70% TCR $^{+}$ hybridomas were discarded.

$\gamma\delta$ T cell hybridomas, derived from naive mouse splenocytes, have previously been shown to spontaneously produce IL-2, a finding that has been interpreted as being due to the expression of a stimulatory ligand for the $\gamma\delta$ TCR by the hybridomas themselves (29, 35). Our hybridomas were therefore tested for the ability to produce IL-2, either spontaneously or after stimulation with anti-CD3. While the hybridomas generally responded to anti-CD3 stimulation, with the levels of IL-2 produced ranging from 274 to 3,629 pg/ml after 24 h of culture, only one line, BC10, produced low levels of IL-2 in the absence of any exogenous stimulation (Table I). The reason for this discrepancy with previously published data is not known but may stem from the fact that our panel of hybridomas was derived from splenocytes of *Listeria*-infected rather than naive, noninfected mice.

Enrichment of Peritoneal Macrophages by Discontinuous Density Centrifugation. PECs to be tested for the ability to stimulate $\gamma\delta$ T cell hybridomas were isolated from either noninfected wild-type mice or mice infected with 2×10^4 CFU *Listeria* 6 d previously, at which time the $\gamma\delta$ T cell response was at its peak (25). PECs were separated over discontinuous Percoll gradients, and fractions of increasing density were collected at the interfaces of each Percoll layer (43, 48, 58, and 63%, and pellet), with the cellular fractions being identified according to the density of Percoll to which they migrated after centrifugation.

PEC fractions were analyzed by flow cytometry to identify their cellular composition (Fig. 3). PECs from uninfected, wild-type mice were comprised predominantly of a mixture of monocytes, macrophages, and B cells, with a minor component of $\gamma\delta$ T cells (Fig. 3 A). Fractionation of PECs from naive mice did not result in a significant enrichment for any cellular component, although the cell yields for the 43 and 48% fractions were very low. In contrast, PECs from 6 d *Listeria*-infected mice were predominantly

comprised (80–90%) of cells of the monocyte/macrophage lineage, based on the expression of the Mac-1 and/or F4/80 markers. Fractionation of these cells resulted in an enrichment for Mac-1⁺ cells in the 43 and 48% fractions, whereas the 58% fraction was comprised mainly of a mixture of Mac-1⁺ cells and B220⁺ cells (B cells). The 63% PEC fraction contained mostly B cells and $\gamma\delta$ T cells, whereas Mac-1⁺ cells represented only a small subset of this population. This fraction also contained the highest proportion of $\gamma\delta$ T cells. The pellet consisted of granulocytes, erythrocytes, and dead cells.

Although the 43, 48, and 58% PEC fractions consisted mainly of cells of the macrophage lineage and expressed similar levels of Mac-1 and F4/80, there were marked differences in their morphology (Fig. 3 B). The 43% PEC fraction was enriched for a distinct population of activated macrophages characterized by large vacuoles and a “foamy” cytoplasm. The 48% PEC fraction also contained large, foamy macrophages, but large vacuolar or apoptotic cells were absent. The 58% fraction of cells contained predominantly monocytes and lymphocytes (B cells). Mature macrophages were essentially absent from this fraction. No *Listeria* organisms could be identified in any of the PEC fractions, and no viable *Listeria* were cultured from lysates of PECs at this stage of the infection, although the livers of these mice still contained viable *Listeria* (data not shown). Thus, as seen previously (30, 36), centrifugation of PECs over discontinuous Percoll gradients resulted in their frac-

tionation into distinct populations of cells with marked differences in maturation and activation.

Stimulation of $\gamma\delta$ T Cell Hybridomas by *Listeria*-elicited PECs. The ability of each of the PEC fractions to stimulate $\gamma\delta$ T cell hybridomas was tested by coculturing the two cell populations for 48 h. Activation of the hybridomas was assessed by two criteria: production of IFN- γ , which has previously been shown to be produced by $\gamma\delta$ T cells after infection with *Listeria* (33), and acquisition of a blast morphology defined by an increase in size and granularity and measured by light scatter properties of the cells. As some cells (e.g., NK cells) present in the PEC fractions were also capable of producing IFN- γ in response to *Listeria* infection in vivo, IFN- γ production by the hybridomas was determined directly by intracellular cytokine staining. Hybridomas were labeled with 5 μ M of the inert fluorescent dye CFSE before culture to distinguish them from PECs. Monensin (2 μ M) was added for the last 4 h of culture to block secretion of newly synthesized IFN- γ . Flow cytometric analysis was then carried out on CFSE⁺ cells. Although some Mac-1⁺ cells acquired CFSE staining after culture, probably as a result of phagocytic uptake of apoptotic hybridoma cells, the level of fluorescent intensity was significantly lower than the intact and viable hybridomas. Analysis of CFSE⁺ cells was restricted to those cells with uniformly high levels of fluorescence.

Representative data, obtained with the BALB/c-derived hybridoma BC10, is shown in Fig. 4, although similar re-

Table I. $\gamma\delta$ T Cell Hybridomas

Strain	Clone	V γ chain	V δ chain	IL-2 production	
				Media	anti-CD3
					pg/ml
C57BL/6 (TCR- $\beta^{-/-}$)	1F1	V γ 1	V δ 6 λ 12	0*	274 \pm 56
	1F4	V γ 1	V δ 6.3	0	278 \pm 83
	1G6	V γ 1	V δ 6.3	0	3,629 \pm 296
	3B8	V γ 1	V δ 6.3	0	1,784 \pm 148
	3D9	V γ 1	V δ 6.3	0	2,120 \pm 349
	3F11	V γ 1	V δ 6.3	0	1,536 \pm 206
	4D11	V γ 1	V δ 6.3	ND	ND
	4D4	V γ 1	V δ 6 λ 12	ND	ND
	1D6	V γ 1	V δ 4	ND	ND
	1B5	V γ 1	V δ 5	0	2,234 \pm 123
	5F11	V γ 1	V δ 5	0	1,011 \pm 180
BALB/c	BB7	V γ 1	V δ 6.3	0	0
	BC10	V γ 1	V δ 6.3	122 \pm 5	167 \pm 20
	BF6	V γ 1	V δ 6.3	0	0

All $\gamma\delta$ T cell hybridomas were derived from splenocytes of mice infected 6 d previously with 10⁴ CFU *Listeria* i.v. that were fused to the BW 5147 thymoma cell line.

*Below level of detection of the assay (10 pg/ml).

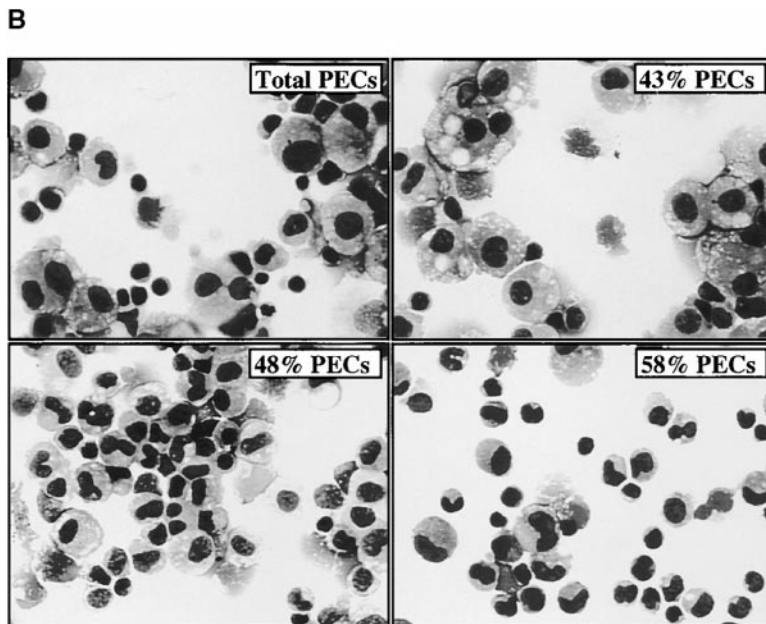
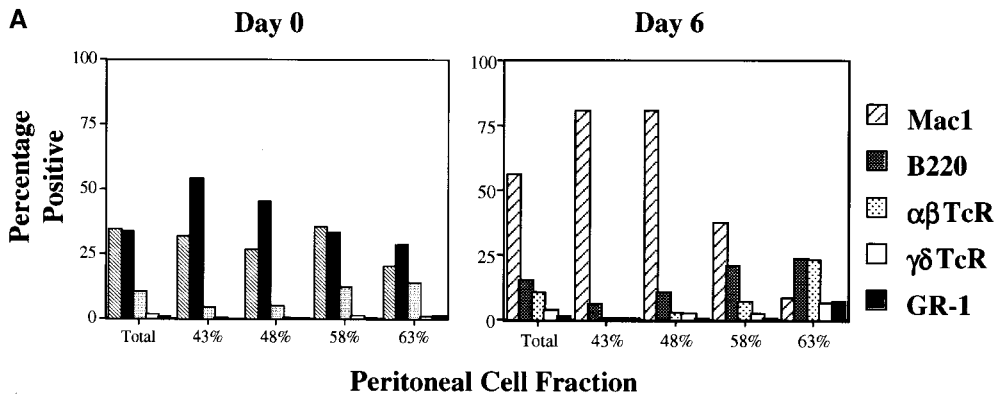


Figure 3. Characterization of PEC fractions from naive and *Listeria*-infected mice. Mice were infected with 2×10^4 CFU *Listeria* intraperitoneally, and PECs were harvested 6 d later. PEC were fractionated over discontinuous Percoll gradients, stained with lineage-specific antibodies, and analyzed by flow cytometry. (A) Composition of PEC fractions before (day 0) and after (day 6) *Listeria* infection. (B) Phenotype of PEC fractions from *Listeria*-infected mice. Cytocentrifuge preparations of Percoll fractions were stained with Wright-Giemsa stain. Magnification 400. The results shown are typical of those obtained from >10 independent experiments.

sults were obtained with nine other hybridomas tested. Hybridomas cultured in the absence of peritoneal cells (Fig. 4 A) or with any of the fractions isolated from naive, non-infected mouse cells did not produce IFN- γ . In the presence of nonseparated PECs from day 6 infected wild-type mice, however, 11% of the hybridoma cells stained positive for IFN- γ . The percentage of IFN- γ -producing hybridomas was further increased to 22% in the presence of the 43% Percoll fraction of PECs, whereas the percentages of IFN- γ -positive hybridomas declined to 8 and 4% in the presence of 48 and 58% Percoll fractions, respectively. By contrast, higher density Percoll fractions were not stimulatory for any of the hybridomas tested. IFN- γ production was dependent upon direct cell-cell contact, as it was not possible to detect any hybridomas stained positive for IFN- γ after transwell culture in which hybridoma cells and PECs were cultured in individual chambers separated by a porous membrane (data not shown). Although the frequency of IFN- γ -secreting $\gamma\delta$ T cells appears to be low, when the proportion of hybridoma cells that have spontaneously lost surface expression of the CD3-TCR complex (20–30%) is taken into account, the frequency of responding (TCR $^+$) cells is higher ($\geq 50\%$). Importantly, IFN- γ synthesis was

restricted to TCRV $\delta 6.3^+$ hybridoma cells, as it was not possible to detect any cytokine synthesis by TCR $^-$ variants isolated from the same cultures or by the parent line BW 5197 TCR- $\alpha^- \beta^-$ (data not shown).

In addition to the production of IFN- γ , stimulated hybridomas also displayed another morphological feature characteristic of cellular activation. The majority of hybridoma cells, when cultured in the presence of low density (43% Percoll fraction) peritoneal macrophages, displayed an increase in size and granularity, as measured by light scatter properties of the cells and compared with hybridomas cultured in the absence of PECs. After culture with unseparated PECs, 20% of the hybridomas had acquired a blast morphology, compared with hybridomas cultured alone (Fig. 4 A). This increased to 68% of hybridomas when cultured with 43% PECs and declined to 24 and 9% when cultured with 48 or 58% PECs, respectively. This blast cell morphology correlated with stimulation, as IFN- γ -positive hybridomas all exhibited a granular phenotype (Fig. 4 B), although a higher percentage of hybridomas exhibited a blast morphology than were stained positive for IFN- γ . The increase in granularity could not be accounted for by increased cellular death of activated cells, as the granular hy-

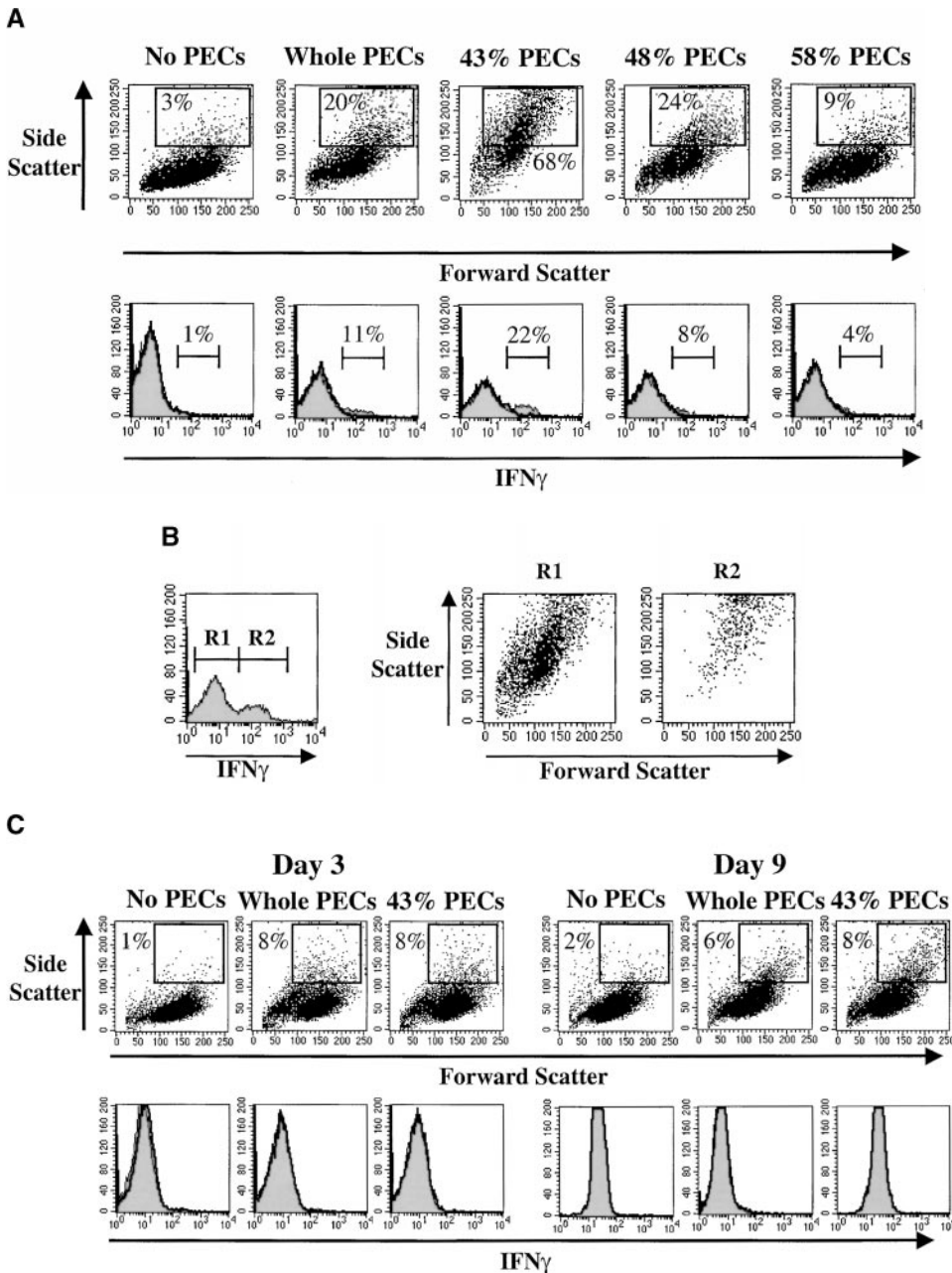


Figure 4. Stimulation of the $\gamma\delta$ T cell hybridoma BC10 by PEC fractions from day 6 *Listeria*-infected mice. 5×10^4 BC10 cells were labeled with CFSE, cultured with 10^5 cells from each of the PEC fractions, isolated from wild-type mice, for 48 h, incubated with monensin for 4 h, and then stained for intracellular IFN- γ before flow cytometry. (A) Flow cytometric analysis of BC10 cells after culture with PEC fractions. Light scatter properties and synthesis of IFN- γ by $\gamma\delta$ T cell hybridomas was determined by electronically gating on CFSE⁺ cells. The percentage values shown for the histogram plots represent the frequency of IFN- γ -producing cells determined by comparing the level of intracellular staining obtained with an isotype-matched control antibody (dark solid lines and open plots) and the anti-IFN- γ antibody (light solid lines and filled-in plots). Similar results were obtained using nine other hybridoma lines. (B) IFN- γ -producing hybridoma cells exhibit blast-like morphology. Electronically gated CFSE⁺ cells were analyzed for IFN- γ synthesis, and the light scatter properties of cells that do (R2) or do not (R1) produce IFN- γ were compared. Note the uniform increase in granularity (SSC) and size (FSC) of IFN- γ -producing cells (R2). The results shown are representative of those obtained from six independent experiments. (C) Flow cytometric analysis of BC10 hybridomas after culture with PECs from day 3 or 9 *Listeria*-infected wild-type mice. Hybridomas were labeled with CFSE before culture, and light scatter properties and synthesis of IFN- γ by $\gamma\delta$ T cell hybridomas was determined by electronically gating on CFSE⁺ cells. The proportion of hybridomas with increased FSC and SSC after culture with PECs is shown in the gated population. The results shown are typical of those obtained from >10 independent experiments.

bridomas were viable at the end of the culture period, as assessed by the ability to exclude vital dyes such as PI (results not shown). The acquisition of a blast-like morphology by the $\gamma\delta$ T cell hybridomas is consistent with the observation that splenic $\gamma\delta$ T cells isolated from *Listeria*-infected mice also demonstrate an increased size and granularity compared with $\gamma\delta$ T cells from noninfected mice (27).

Stimulation of the hybridomas was maximal when PECs were harvested from day 6 infected mice, as whole PECs harvested from noninfected or from infected mice at day 3 or 9 after infection failed to stimulate IFN- γ production by the hybridomas (Fig. 4 C). Similarly, the 43% Percoll frac-

tion from day 3 or 9 infected mice was also unable to induce IFN- γ production by the hybridoma cells. Bulk PECs or the 43% Percoll-enriched fraction from both day 3 and day 9 infected mice, however, were weakly stimulatory in that they induced an increase in size and granularity of a small proportion (<10%) of hybridoma cells. The kinetics of the generation of $\gamma\delta$ T cell-reactive macrophages corresponded with the peak in $\gamma\delta$ T cell expansion and IFN- γ production seen in vivo after intraperitoneal infection with *Listeria* (25, 33). In addition, no MHC restriction was seen in the ability of the 43% PECs to stimulate the hybridomas, as C57BL/6- or BALB/c-derived hybridomas could be

stimulated equally well with PECs isolated from either strain (data not shown). This is in agreement with previous results demonstrating no MHC requirement for $\gamma\delta$ T cell activation (37).

Activated Macrophages Stimulate $\gamma\delta$ T Cell Hybridomas. 6 d after infection, cells recovered in the 43% Percoll fraction of wild-type PECs represent between 2 and 4% of the total PECs recovered from individual mice. Wright-Giemsa staining of cytocentrifuge preparations of the 43% Percoll fraction of *Listeria*-elicited PECs identified the majority ($\geq 60\%$) as being large, mature activated macrophages (Fig. 3 B), although light scatter analysis by flow cytometry showed two distinct populations of macrophages within this fraction (Fig. 5). One of these populations contained cells with moderate to high side scatter and low forward scatter (H-SSC/L-FSC; R1 in Fig. 5 A). Of note, this H-SSC/L-FSC population, which is difficult to distinguish in whole *Listeria*-elicited PECs, is enriched in the 43% fraction. The second macrophage population comprised cells

with both high forward and side scatter (H-SSC/H-FSC; R2 in Fig. 5 A). Both populations expressed Mac-1 and F4/80 antigens, although the H-SSC/H-FSC population expressed slightly higher levels of Mac-1 (mean fluorescence intensity of 1,821 for the H-SSC/H-FSC cells, compared with 1,082 for the H-SSC/L-FSC cells). To determine the ability of each subpopulation to stimulate $\gamma\delta$ T cell hybridomas, the macrophage subpopulations of the 43% Percoll fraction were further separated by flow cytometric sorting based upon their different light scatter properties.

Although the two populations of macrophages expressed similar levels of Mac-1 and F4/80 on their surfaces, they differed markedly in appearance (Fig. 5 B). The H-SSC/L-FSC (R1) cells appeared to be active phagocytic cells, containing numerous large vacuoles within the cytoplasm. In contrast, the H-SSC/H-FSC (R2) macrophages generally had a smaller, granular cytoplasm in which the large vacuoles were noticeably absent. To assess the ability of each

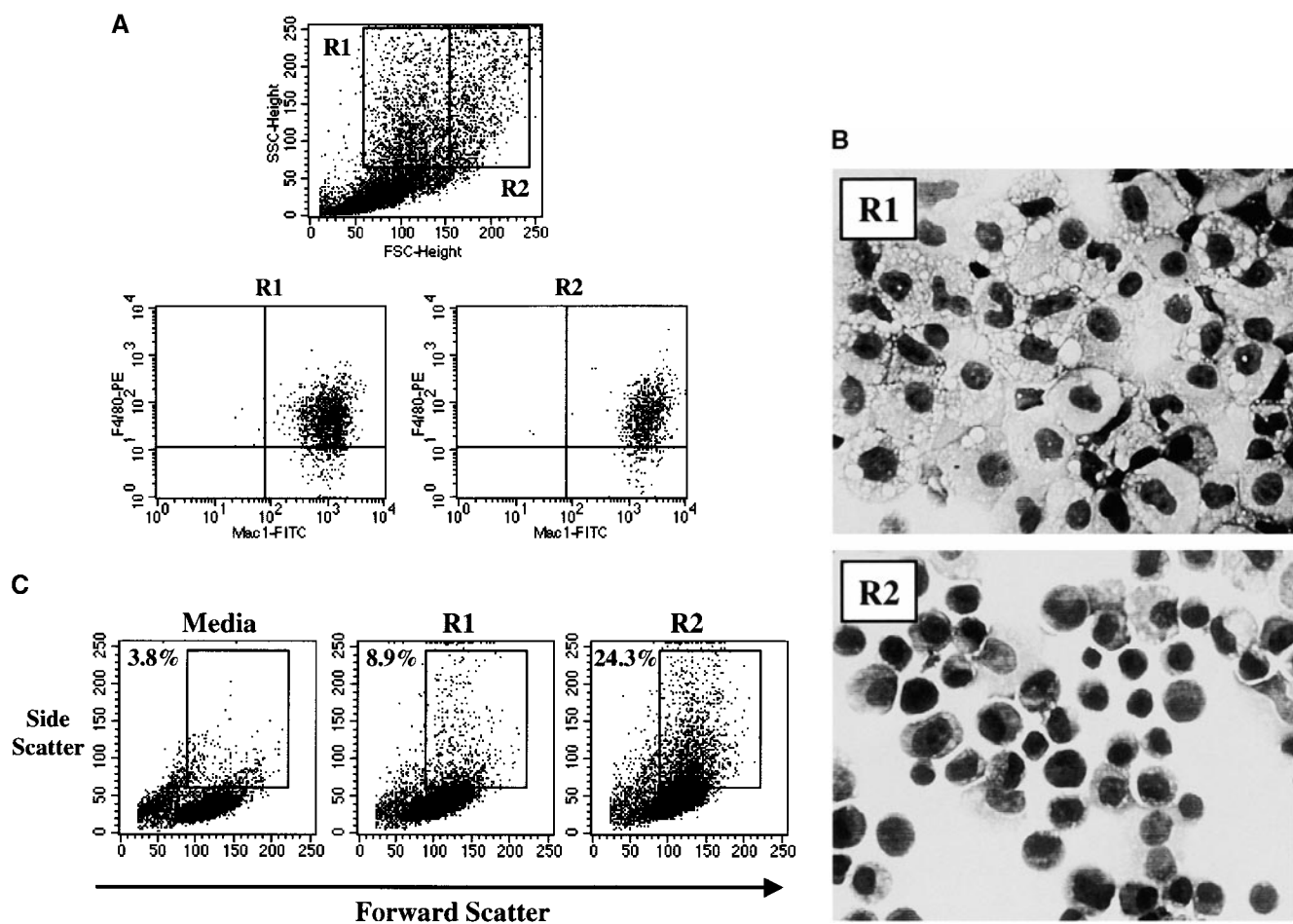


Figure 5. Stimulation of $\gamma\delta$ T cells hybridomas by sorted subsets of low density *Listeria*-elicited PECs. (A) Two distinct populations of macrophages (R1 and R2) were separated from the low density (43%) Percoll fraction of PECs from mice infected 6 d previously with *Listeria* by their light scatter properties (FSC and SSC). Each population was reanalyzed for expression of macrophage markers Mac-1 and F4/80 (lower panels). (B) Cytocentrifuge preparations of sorted populations (Wright-Giemsa stain; magnification 400). (C) Stimulation of $\gamma\delta$ T cell hybridomas by sorted subsets. Hybridomas were labeled with CFSE and cultured for 24 h in the presence of media alone, unsorted low density PECs (43% PECs), or the sorted PEC populations (R1 and R2). Hybridoma stimulation was assessed by the change in cellular morphology, detected by light scatter properties of CFSE⁺ cells. The percentage of cells exhibiting a blast-like morphology (increased SSC) are shown.

sub-population of macrophages to stimulate $\gamma\delta$ T cells, hybridomas were labeled with CFSE before culture, and activation was assessed by the acquisition of a blast-like morphology based on the light scattering properties of the green fluorescent cells (Fig. 5 C). Stimulation of the hybridomas with sorted populations of the H-SSC/H-FSC (R2) population of macrophages resulted in 24% of the cells developing a blast cell-like morphology, compared with <4% of the hybridomas when cultured alone. By contrast, significantly lower levels of $\gamma\delta$ T cell activation were seen in cultures containing H-SSC/L-FSC (R1) macrophages. Thus, the H-SSC/H-FSC macrophage population is enriched for cells capable of activating the $\gamma\delta$ T cell hybridomas. Other than differences in the ability to stimulate $\gamma\delta$ T cell hybridomas, we have been unable to distinguish between the H-SSC/H-FSC and H-SSC/L-FSC macrophage subpopulations using cell surface markers such as MHC class I and II, B7-1, and B7-2 or hsp60.

Lysis of Activated Macrophages by $\gamma\delta$ T Cells In Vitro. Collectively, the above data demonstrates that $\gamma\delta$ T cells interact with activated macrophages in vivo after infection and that, in the absence of $\gamma\delta$ T cells, there is a defect in the apoptotic death and removal of these cells. This suggests that $\gamma\delta$ T cells are cytotoxic for activated macrophages.

To directly demonstrate cytotoxicity of $\gamma\delta$ T cells for activated macrophages, an in vitro ^{51}Cr -release assay was carried out. Target cells were low and high density macrophages obtained from PECs of TCR- $\delta^{-/-}$ mice infected with *Listeria* 6 d previously. Low density macrophages were collected at the 43% Percoll interface, and higher density cells were collected from the pellet. Targets were labeled in vitro with ^{51}Cr for 2 h before culture. For these experiments, primary splenic $\gamma\delta$ T cells were used as effectors, as we were unable to demonstrate lysis of macrophages in preliminary experiments using $\gamma\delta$ T cell hybridomas as effector cells. This could have been due to a loss of cytotoxic activity of the hybridomas in culture, as hybridomas were routinely maintained according to expression of the $\gamma\delta$ TCR rather than cytolytic activity or any other effector functions. To enrich for $\gamma\delta$ effector cells, splenocytes from day 6 infected C57BL/6 wild-type and TCR- $\beta^{-/-}$ mice were depleted of B cells, myeloid cells, and $\alpha\beta$ T cells by negative immunomagnetic selection. In addition, splenocytes from day 6 infected TCR- $\delta^{-/-}$ mice were similarly treated to enrich for any non-T cell-derived (i.e., NK cell) cytotoxic activity. Effector cells from wild-type and TCR- $\beta^{-/-}$ splenocytes comprised $\sim 70\%$ $\gamma\delta$ T cells, of which V $\delta 6^+$ cells represented between 60 and 80% of TCR- $\gamma\delta^+$ cells (data not shown). The contaminating cells were primarily B cells and $\alpha\beta$ T cells in the $\gamma\delta$ T cell preparations from wild-type spleen cells and B cells in the $\gamma\delta$ T cell-enriched preparations from TCR- $\beta^{-/-}$ mice. The effector cells obtained from TCR- $\delta^{-/-}$ splenocytes were primarily (>60%) NK cells and contaminating B cells. ^{51}Cr release was measured after 16-h coculture of target and effector cells.

Low density macrophages from TCR- $\delta^{-/-}$ mice were efficiently lysed by $\gamma\delta$ T cell-enriched splenocytes of wild-type and TCR- $\beta^{-/-}$ mice, but not TCR- $\delta^{-/-}$ mice (Fig. 6

A). The absence of any killing activity among day 6 infected TCR- $\delta^{-/-}$ splenocytes depleted of myeloid and B and T cells also excludes the possibility that macrophage cytotoxic activity is mediated by other non-T cell subpopulations such as NK cells. In addition, there was no significant lysis of low density PECs by nylon wool-purified T cells from day 6 infected wild-type mice, which comprised >90% $\alpha\beta$ T cells at E/T ratios as high as 20:1, essentially excluding the possibility that the cells cytotoxic for macrophage were (CD8) $\alpha\beta$ T cells. To determine if $\gamma\delta$ T cell cytotoxicity was restricted to low density PECs, the assay was repeated using high density PECs that were pelleted after centrifugation over 43% Percoll (Fig. 6 B). Effector cells were splenocytes from wild-type mice enriched for $\gamma\delta$ T cells or TCR- $\delta^{-/-}$ splenocytes depleted of B cells, $\alpha\beta$ T cells, and myeloid cells as described above. Although $\gamma\delta$ T cell-enriched splenocytes from wild-type mice were able to lyse low density macrophages, no specific lysis was seen when higher density cells were used as targets (Fig. 6 B). These cells were also unable to stimulate the $\gamma\delta$ T cell hybridomas (Fig. 4), consistent with a need for $\gamma\delta$ T cell activation for the induction of cytotoxicity.

To determine if cytotoxic activity of $\gamma\delta$ T cells against low density macrophages occurred after signaling through the $\gamma\delta$ TCR, the assay was repeated in the presence of increasing concentrations of F(ab) $_2$ fragments of the mAb GL3, specific for the $\gamma\delta$ TCR. F(ab) $_2$ fragments, rather than whole antibody, were used to avoid the possibility that binding of the antibody to macrophage Fc receptors could induce $\gamma\delta$ T cell activation through cross-linking of the TCR rather than block cytotoxicity. Lysis of low density macrophages by $\gamma\delta$ T cells was effectively abolished in the presence of F(ab) $_2$ fragments of GL3 antibody at concentrations as low as 2 $\mu\text{g}/\text{ml}$. In contrast, the inclusion of F(ab) $_2$ fragments of hamster IgG did not interfere with $\gamma\delta$ T cell cytotoxicity. These results are consistent with a requirement for signaling through the $\gamma\delta$ TCR for cytotoxic activity to be induced.

Collectively, these results demonstrate that primary $\gamma\delta$ T cells, activated as a result of *Listeria* infection in vivo, selectively kill low density macrophages.

Discussion

This study describes a novel interaction between $\gamma\delta$ T cells and low density macrophages, isolated at the later stages of an immune response to infection in which $\gamma\delta$ T cells are activated by macrophages and, in turn, acquire cytotoxic activity to eliminate the stimulatory macrophage. In the absence of $\gamma\delta$ T cells in vivo, the elimination of macrophages is impaired, resulting in the accumulation of activated macrophages at sites of infection. The ability of $\gamma\delta$ T cells to lyse various tumor cell lines, such as the Daudi Burkitt's lymphoma cell line, or macrophages infected in vitro with *Mtb* or *Toxoplasma gondii* has been previously described (14, 38). To our knowledge, however, this is the first report demonstrating stimulation in vivo of $\gamma\delta$ T cells by primary, nontransformed cells occurring as part of a co-

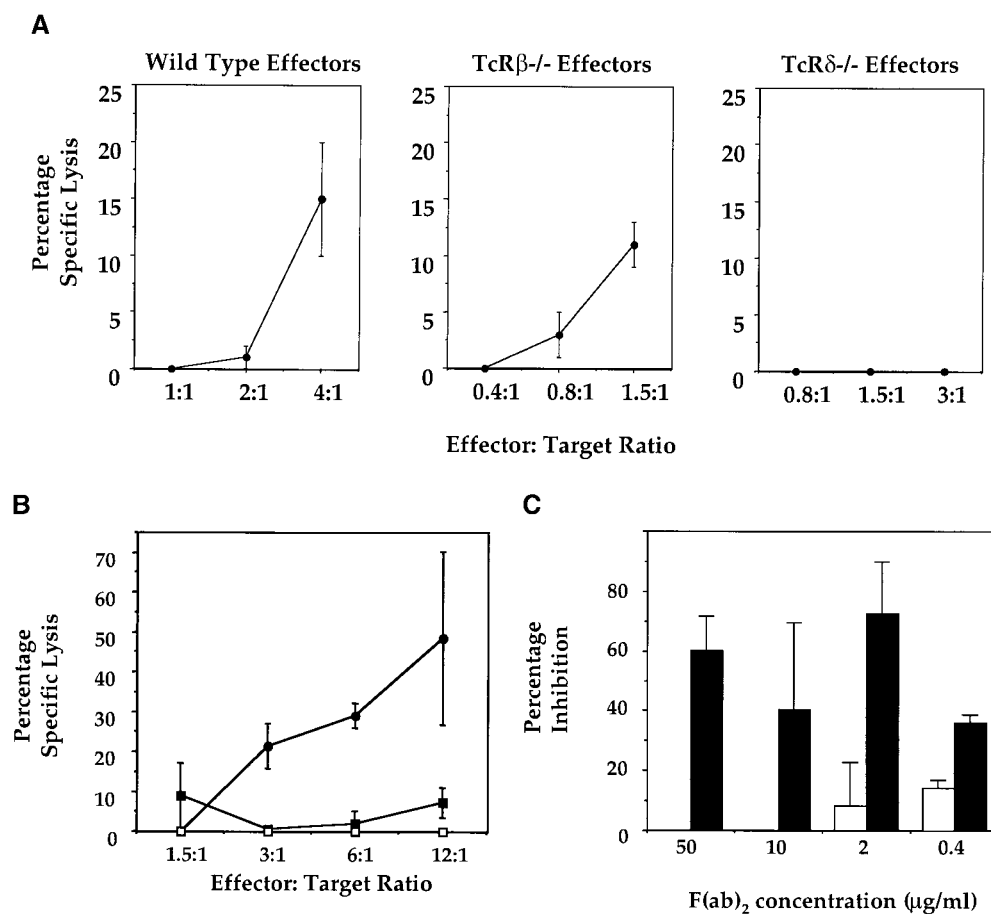


Figure 6. Cytolytic activity of splenocytes enriched for $\gamma\delta$ T cells. (A) PECs from day 6 infected TCR- $\delta^{-/-}$ mice were separated by centrifugation over 43% Percoll to obtain low density PECs and labeled with ^{51}Cr . Labeled target cells were incubated with splenocytes enriched from wild-type, TCR- $\beta^{-/-}$, or TCR- $\delta^{-/-}$ mice. Splenocytes were depleted of B cells, $\alpha\beta$ T cells, and myeloid cells by depletion over immunomagnetic columns to enrich for $\gamma\delta$ T cells. (B) Cytolytic activity of $\gamma\delta$ T cell-enriched splenocytes against low density (circles) and high density (squares) PECs. Splenocytes from wild-type (closed symbols) and TCR- $\delta^{-/-}$ (open symbols) mice were cultured with ^{51}Cr -labeled PECs. Targets were isolated by centrifugation over 43% Percoll to obtain low density (circles) and high density (squares) PECs. (C) Cytolytic activity of $\gamma\delta$ T cell-enriched splenocytes against ^{51}Cr -labeled low density PECs in the presence of F(ab)₂ fragments of hamster Ig (open bars) or GL3 (anti $\gamma\delta$ TCR; solid bars) mAb. Cells were cultured at an E/T ratio of 10:1. Results are expressed as percent inhibition, calculated according to the formula: percent inhibition = [(percent lysis with no antibody) - percent lysis with antibody] / percent lysis with no antibody \times 100%. Data are expressed as the mean and SE of triplicate cultures.

ordinated immune response to infectious challenge and provides evidence for $\gamma\delta$ T cells being involved in macrophage homeostasis at the conclusion of an inflammatory response. These results are consistent with a model in which $\gamma\delta$ T cells are responsible for inducing cell death in activated macrophages and, in the process, promote the resolution of inflammation after the termination of the immune response to *Listeria*.

Infection of mice with *Listeria* induces a pronounced increase in the production and activation of monocytes and macrophages at the site of infection, which, in turn, results in bacterial clearance. To maintain macrophage homeostasis, however, most if not all of the macrophages generated in response to the infection must be removed after clearance of bacteria. The decreased cell death and accumulation of activated, low density macrophages seen in the peritoneum of *Listeria*-infected TCR- $\delta^{-/-}$ mice is consistent with an active role for $\gamma\delta$ T cells in this process. One possible scenario is that activated macrophages may upregulate stimulatory ligands for the $\gamma\delta$ TCR at the late phase of an immune response, resulting in $\gamma\delta$ T cell stimulation and

acquisition of cytotoxic activity. This is consistent with the kinetics of hybridoma stimulation by PECs derived from mice over the course of infection, which is maximal at day 6 after infection. At earlier time points, activated macrophages are required to control the growth of bacteria, so negative regulatory mechanisms to eliminate these cells or inhibit their activity would be deleterious to the animal. By day 6, however, when the bacteria have been contained or eliminated, the persistence of inflammatory macrophages could lead to tissue damage through the production of toxic inflammatory mediators, necessitating their removal. By 9 d after infection, the stimulatory macrophages have been cleared, returning the animal to a state of normal homeostasis. This model is consistent with previous reports describing proliferation of human $\gamma\delta$ T cells in response to macrophages infected with Mtb or mycobacterial extracts and the ability of $\gamma\delta$ T cells to lyse macrophages infected in vitro with Mtb (39, 40). Although we have not determined the mechanism by which $\gamma\delta$ T cells kill activated macrophages, examples of cytotoxicity induced by $\gamma\delta$ T cells through both the perforin pathway as well as through ligu-

tion of Fas on target cells have been reported (41, 42). In preliminary experiments to address this question, however, cytotoxicity of macrophages by $\gamma\delta$ T cells was enhanced in the presence of EDTA, which inhibits the metalloproteinase-dependent cleavage of TNF superfamily members such as Fas ligand or TNF- α . Conversely, an inhibitor of perforin activity, concanamycin A, had no effect on $\gamma\delta$ T cell cytotoxic activity (our unpublished observations).

The decreased necrosis and accumulation of macrophages in the peritoneum contrasts with the appearance of necrotic lesions in the liver. However, the liver pathology described for TCR- $\delta^{-/-}$ mice after infection with *Listeria* is consistent with our model. Persistence of activated macrophages at sites of infection, including the liver, could result in excessive production of toxic products, including proinflammatory cytokines, reactive oxygen and nitrogen mediators, and proteolytic enzymes (5). In fixed tissue sites, such as the liver, this would lead to cellular damage and necrosis of adjacent hepatocytes. The presence of necrotic hepatocytes could then induce secondary inflammation, characterized by an influx of neutrophils into the lesion. In the peritoneum, where the inflammatory cells are not directly adjacent to other cells, necrosis of adjoining cells would be less likely to occur. The predominance of activated macrophages in livers and the spleens of infected TCR- $\delta^{-/-}$ mice and the finding that $\gamma\delta$ T cells are found in close association with macrophages in the spleens and livers of infected wild-type mice (Egan, P.J., R.L. Nosheny, A. Kuhl, and S.R. Carding, manuscript in preparation) is consistent with the $\gamma\delta$ T cells being involved in macrophage homeostasis and that the exaggerated inflammatory response and liver necrosis present in infected TCR- $\delta^{-/-}$ mice is a consequence of the inability to eliminate activated macrophages. Necrotic lesions have also been identified in the lungs of TCR- $\delta^{-/-}$ mice infected with Mtb, even when low inoculating doses of bacteria were used (18). This suggests that the dysregulation of inflammation seen in TCR- $\delta^{-/-}$ mice is not limited to the response to *Listeria* but rather may be generally applicable for all responses for this population of $\gamma\delta$ T cells.

Although the nature of the stimulatory ligand expressed by the activated macrophages has not been addressed in this study, the $\gamma\delta$ T cell response could be driven either by a bacterial-derived antigen, an autologous antigen induced as a result of infection, or a combination of the two. Candidate molecules include endogenous or pathogen-derived hsp60. Mycobacterial hsp60 has been demonstrated to activate V γ 1/V δ 6 T cells (29), a receptor combination expressed by the same population of cells that respond to infection with *Listeria* (27) and by the majority of hybridomas described here. We have recently shown expression of autologous hsp60 on the plasma membranes of cells, including macrophages, taken from the site of *Listeria* infection (34) and that $\gamma\delta$ (V δ 6⁺) T cells colocalize with hsp60⁺ macrophages in tissue of infected mice (Kuhl, A., and S.R. Carding, unpublished observations). Expression of autologous plasma membrane hsp60 also correlated with the expansion of $\gamma\delta$ T cells in vivo, consistent with the hypothe-

sis that $\gamma\delta$ T cells were responding to this antigen. Although we cannot rule out the possibility that $\gamma\delta$ T cells are recognizing listerial antigens presented by the macrophages, presentation of these antigens does not involve MHC class I or II presentation pathways, as hybridoma stimulation occurred in the presence of an MHC mismatch between the stimulator and responder cells. This is consistent with published data demonstrating no requirement for classical MHC class I or II antigen processing or presentation for $\gamma\delta$ T cell reactivity (37).

The possibility that $\gamma\delta$ T cells are responsible for maintaining macrophage homeostasis after an immune response has obvious implications for human inflammatory disorders in which there is an involvement of $\gamma\delta$ T cells. For instance, we have demonstrated that a loss of $\gamma\delta$ T cells, through Fas-FasL induced apoptosis, in the lungs of patients with tuberculosis is associated with poor prognosis and disease progression characterized by the accumulation of activated, inflammatory macrophages that produce high levels of TNF- α (43, 44). This is consistent with our model in which murine $\gamma\delta$ T cells limit the extent of macrophage activation in response to infection. Loss of $\gamma\delta$ T cells capable of killing Mtb-infected macrophages (39) would, therefore, result in dysregulation of macrophage activation and the sustained production of inflammatory mediators that contribute to the pathophysiology of advanced pulmonary tuberculosis.

In summary, our findings presented here provide, for the first time, evidence for an interaction between $\gamma\delta$ T cells and activated macrophages during the cellular immune response to microbial infection. They provide in vivo evidence for $\gamma\delta$ T cell-mediated cytotoxicity as a means of maintaining macrophage homeostasis after the termination of the response to infection.

We thank Drs. Phil Scott and Chris Hunter for critical review of the manuscript.

This work was supported by Public Health Service grants AI-31972, AI-45993, and HL-51749 from the National Institutes of Health, by grant RPG-97-027 from the American Cancer Society, and by a grant from the University of Pennsylvania Research Foundation.

Submitted: 26 January 2000

Revised: 19 April 2000

Accepted: 27 April 2000

References

1. Small, P.L.C., L. Ramakrishnan, and S. Falkow. 1994. Remodeling schemes of intracellular pathogens. *Science*. 263: 637–639.
2. Solbach, W., H. Moll, and M. Rollinghoff. 1991. Lymphocytes play the music but macrophages call the tune. *Immunol. Today*. 12:4–6.
3. Adams, D.O., and T.A. Hamilton. 1992. Macrophages as destructive cells in host defense. In *Inflammation: Basic Principles and Clinical Correlates*. J.I. Gallin, I.M. Goldstein, and R. Snyderman, editors. Raven Press, New York. 673–691.
4. Khalil, N., O. Berezny, M. Sporn, and A.H. Greenberg.

1989. Macrophage production of transforming growth factor beta and fibroblast collagen synthesis in chronic pulmonary inflammation. *J. Exp. Med.* 170:727–733.
5. Nathan, C.F. 1987. Secretory products of macrophages. *J. Clin. Invest.* 79:319–326.
 6. Robertson, O.H., and C.G. Uhlley. 1938. Changes occurring in the macrophage system of the lungs in pneumococcus lobar pneumonia. *J. Clin. Invest.* 15:115–130.
 7. Albina, J.E., S. Cui, R.B. Mateo, and J.S. Reichner. 1993. Nitric oxide-mediated apoptosis in murine peritoneal macrophages. *J. Immunol.* 150:5080–5086.
 8. Khelef, N., A. Zychlinsky, and N. Guiso. 1993. *Bordetella pertussis* induces apoptosis in macrophages: role of adenylate cyclase-hemolysin. *Infect. Immun.* 61:4064–4069.
 9. Mangan, D.F., and S.M. Wahl. 1991. Differential regulation of human monocyte programmed cell death (apoptosis) by chemotactic factors and pro-inflammatory cytokines. *J. Immunol.* 147:3408–3413.
 10. Zychlinsky, A., M.C. Pravost, and P.J. Sansonetti. 1992. *Shigella flexneri* induces apoptosis in infected macrophages. *Nature.* 358:167–169.
 11. Bellingan, G.J., H. Caldwell, S.E.M. Howie, I. Dransfield, and C. Haslett. 1996. In vivo fate of the inflammatory macrophage during the resolution of inflammation: inflammatory macrophages do not die locally, but emigrate to the draining lymph nodes. *J. Immunol.* 157:2577–2585.
 12. Carding, S.R., W. Allan, S. Kyes, A. Hayday, K. Bottomly, and P.C. Doherty. 1990. Late dominance of the inflammatory process in murine influenza by γ/δ^+ T cells. *J. Exp. Med.* 172:1225–1231.
 13. Hou, S., J.M. Katz, P.C. Doherty, and S.R. Carding. 1992. Extent of $\gamma\delta$ T cell involvement in the pneumonia caused by Sendai virus. *Cell. Immunol.* 143:183–193.
 14. Kasper, L.H., T. Matsuura, S. Fonseka, J. Arruda, J.Y. Channon, and I.A. Khan. 1996. Induction of gamma delta T cells during acute murine infection with *Toxoplasma gondii*. *J. Immunol.* 157:5521–5527.
 15. van der Heyde, H.C., M.M. Elloso, W.L. Chang, M. Kaplan, D.D. Manning, and W.P. Weidanz. 1995. Gamma delta T cells function in cell-mediated immunity to acute blood-stage *Plasmodium chabaudi adami* malaria. *J. Immunol.* 154:3985–3990.
 16. Fu, Y.X., C.E. Roark, K. Kelly, D. Drevets, P. Campbell, R. O'Brien, and W. Born. 1994. Immune protection and control of inflammatory tissue necrosis by $\gamma\delta$ T cells. *J. Immunol.* 153:3101–3115.
 17. Mombaerts, P., J. Arnoldi, F. Russ, S. Tonegawa, and S.H.E. Kaufmann. 1993. Different roles of $\alpha\beta$ and $\gamma\delta$ T cells in immunity against an intracellular bacterial pathogen. *Nature.* 365:53–56.
 18. D'Souza, C.D., A.M. Cooper, A.A. Frank, R.J. Mazzaccaro, B.R. Bloom, and I.M. Orme. 1997. An anti-inflammatory role for gamma delta T lymphocytes in acquired immunity to *Mycobacterium tuberculosis*. *J. Immunol.* 158:1217–1221.
 19. Roberts, S.J., A.L. Smith, A.B. West, L. Wen, R.C. Findly, M.J. Owen, and A.C. Hayday. 1996. T cell alpha beta and gamma delta deficient mice display abnormal but distinct phenotypes toward a natural, widespread infection of the intestinal epithelium. *Proc. Natl. Acad. Sci. USA.* 93:11774–11779.
 20. Peng, S.L., M.P. Madaio, A.C. Hayday, and J. Craft. 1996. Propagation and regulation of systemic autoimmunity by $\gamma\delta$ T cells. *J. Immunol.* 157:5689–5698.
 21. Bucht, A., K. Soderstrom, T. Hultman, M. Uhlen, E. Nilsson, R. Kiessling, and A. Gronberg. 1992. T cell receptor diversity and activation markers in the V delta 1 subset of rheumatoid synovial fluid and peripheral blood T lymphocytes. *Eur. J. Immunol.* 22:567–574.
 22. Mukasa, A., M. Lahn, E.K. Pflum, W. Born, and R.L. O'Brien. 1997. Evidence that the same $\gamma\delta$ T cells respond during infection-induced and autoimmune inflammation. *J. Immunol.* 159:5787–5794.
 23. Unanue, E.R. 1997. Studies in listeriosis show the strong symbiosis between the innate cellular system and the T cell response. *Immunol. Rev.* 158:11–25.
 24. Hiromatsu, K., G. Yoshikai, G. Matsuzaki, S. Ohga, K. Muramori, K. Matsumoto, J.A. Bluestone, and K. Nomoto. 1992. A protective role of γ/δ T cells in primary infection with *Listeria monocytogenes*. *J. Exp. Med.* 175:49–56.
 25. Skeen, M.J., and H.K. Ziegler. 1993. Induction of murine peritoneal γ/δ T cells and their role in resistance to bacterial infection. *J. Exp. Med.* 178:971–984.
 26. Ohga, S., Y. Yoshikai, Y. Takeda, K. Hiromatsu, and K. Nomoto. 1990. Sequential appearance of $\gamma\delta$ and $\alpha\beta$ bearing T cells in the peritoneal cavity during an i.p. infection with *Listeria monocytogenes*. *Eur. J. Immunol.* 20:533–538.
 27. Belles, C., A.L. Kuhl, A.J. Donoghue, Y. Sano, R.L. O'Brien, W. Born, K. Bottomly, and S.R. Carding. 1996. Bias in the $\gamma\delta$ T cell response to *Listeria monocytogenes*: V δ 6.3⁺ cells are a major component of the $\gamma\delta$ T cell response to *Listeria monocytogenes*. *J. Immunol.* 156:4280–4289.
 28. Haas, W., P. Pereira, and S. Tonegawa. 1993. Gamma/delta cells. *Annu. Rev. Immunol.* 11:637–685.
 29. O'Brien, R.L., Y.X. Fu, R. Cranfill, A. Dallas, C. Ellis, C. Readon, J. Lang, S.R. Carding, R. Kubo, and W. Born. 1992. Heat shock protein Hsp60-reactive $\gamma\delta$ T cells: a large diversified T-lymphocyte subset with highly focused specificity. *Proc. Natl. Acad. Sci. USA.* 89:4348–4352.
 30. Vray, B., and N. Plasman. 1994. Separation of murine peritoneal macrophages using percoll density gradients. *J. Immunol. Methods.* 174:53–59.
 31. Assenmacher, M., J. Schmitz, and A. Radbruch. 1994. Flow cytometric determination of cytokines in activated murine T helper lymphocytes: expression of interleukin-10 in interferon-gamma and in interleukin-4-expressing cells. *Eur. J. Immunol.* 24:1097–1101.
 32. Lyons, A.B., and C.R. Parish. 1994. Determination of lymphocyte division by flow cytometry. *J. Immunol. Methods.* 171:131–137.
 33. Ferrick, D.A., M.D. Schrenzel, T. Mulvania, B. Hsieh, W.G. Ferlin, and H. Lepper. 1995. Differential production of interferon- γ and interleukin-4 in response to Th1- and Th2-stimulating pathogens by $\gamma\delta$ T cells in vivo. *Nature.* 373:255–257.
 34. Belles, C., A. Kuhl, R. Nosheny, and S.R. Carding. 1999. Plasma membrane expression of heat shock protein 60 (hsp60) in vivo in response to infection. *Infect. Immun.* 67:4191–4200.
 35. O'Brien, R.L., M.P. Happ, A. Dallas, E. Palmer, R. Kubo, and W.K. Born. 1989. Stimulation of a major subset of lymphocytes expressing T cell receptor gamma delta by an antigen derived from *Mycobacterium tuberculosis*. *Cell.* 57:667–674.
 36. DaMatta, R.A., T. Araujo-Jorge, and W. de Souza. 1995. Subpopulations of mouse resident peritoneal macrophages fractionated on Percoll gradients show differences in cell size, lectin binding and antigen expression suggestive of different

- stages of maturation. *Tissue Cell*. 27:505–513.
37. Schild, H., N. Mavaddat, C. Litzenberger, E.W. Ehrlich, M.M. Davis, J.A. Bluestone, L. Matis, R.K. Draper, and Y.H. Chien. 1994. The nature of major histocompatibility complex recognition by $\gamma\delta$ T cells. *Cell*. 76:29–37.
 38. Fisch, P., M. Mlkovsky, S. Kovats, E. Sturm, E. Braakman, B.S. Klein, S.D. Voss, L.W. Morrissey, R. DeMars, W.J. Welch, et al. 1990. Recognition by human V γ 9/V δ 2 T cells of a GroEL homolog on Daudi Burkitt's lymphoma cells. *Science*. 250:1269–1273.
 39. Balaji, K., S.K. Schwander, E.A. Rich, and W.H. Boom. 1995. Alveolar macrophages as accessory cells for human $\gamma\delta$ T cells activated by *Mycobacterium tuberculosis*. *J. Immunol*. 154: 5959–5968.
 40. Munk, M.E., A.J. Gatrill, and S.H.E. Kaufmann. 1990. Target cell lysis and IL-2 secretion by $\gamma\delta$ T lymphocytes after activation with bacteria. *J. Immunol*. 145:2434–2439.
 41. Lin, T., T. Brunner, B. Tietz, J. Madsen, E. Bonfoco, M. Reaves, M. Huflejt, and D.R. Green. 1998. Fas ligand-mediated killing by intestinal intraepithelial lymphocytes. Participation in intestinal graft-versus-host disease. *J. Clin. Invest*. 101:570–577.
 42. Zeine, R., R. Pon, U. Ladiwala, J.P. Antel, L.G. Filion, and M.S. Freedman. 1998. Mechanism of gamma delta T cell-induced human oligodendrocyte cytotoxicity: relevance to multiple sclerosis. *J. Neuroimmunol*. 87:49–61.
 43. Li, B.Q., H. Bassiri, M.D. Rossman, P. Kramer, A.F. Eyuboglu, M. Torres, E. Sada, T. Imir, and S.R. Carding. 1998. Involvement of the Fas/Fas ligand pathway in activation-induced cell death of mycobacteria-reactive human gamma delta T cells: a mechanism for the loss of gamma delta T cells in patients with pulmonary tuberculosis. *J. Immunol*. 161: 1558–1567.
 44. Li, B.Q., M.D. Rossman, T. Imir, A.F. Oner-Eyuboglu, C.W. Lee, R. Biancaniello, and S.R. Carding. 1996. Disease specific changes in $\gamma\delta$ T cell repertoire and function in patients with pulmonary tuberculosis. *J. Immunol*. 157:4222–4229.